Electronic Supplementary Material (ESI) for Journal of Materials Chemistry A.

Synergistic effect of S,N-co-doped Mesoporous Carbon Materials with High Performance for Oxygen-Reduction Reaction and Li-ion Batteries

Gui-lin Zhuang, [†,⊥] *Jia-qi Bai,* [†,⊥] *Xin-yong Tao,* [‡⊥] *Jian-min Luo,* [‡] *Xin-de Wang,* [†] *Yi-fen Gao,* [†] *Xing Zhong,* [†] Xiao-nian Li, [†] *Jian-guo Wang** [†]

[†]Institute of Industrial Catalysis, College of Chemical Engineering, Zhejiang University of Technology, Hangzhou, People's Republic of China, 310032.

[‡] College of Material Science and Engineering, Zhejiang University of Technology, Hangzhou, People's Republic of China, 310032

1. **Structural characterization of SNPC-500, SNPC-600, SNPC-700, SNPC-800 , SPC-800 and NPC-800.**

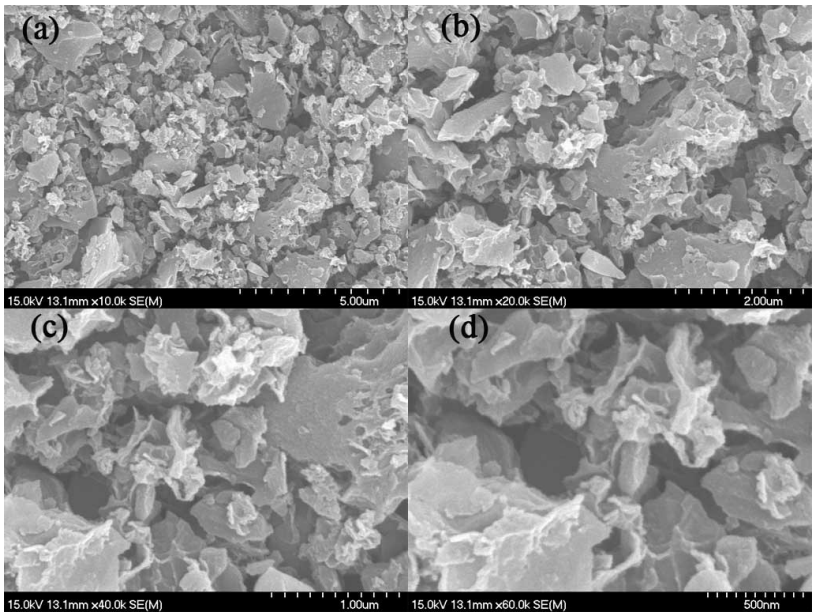

Fig. S1. SEM images of SNPC-800 with a scale bar of 5μm (a) , 2μm (b) ,1μm (c), 500nm(d).

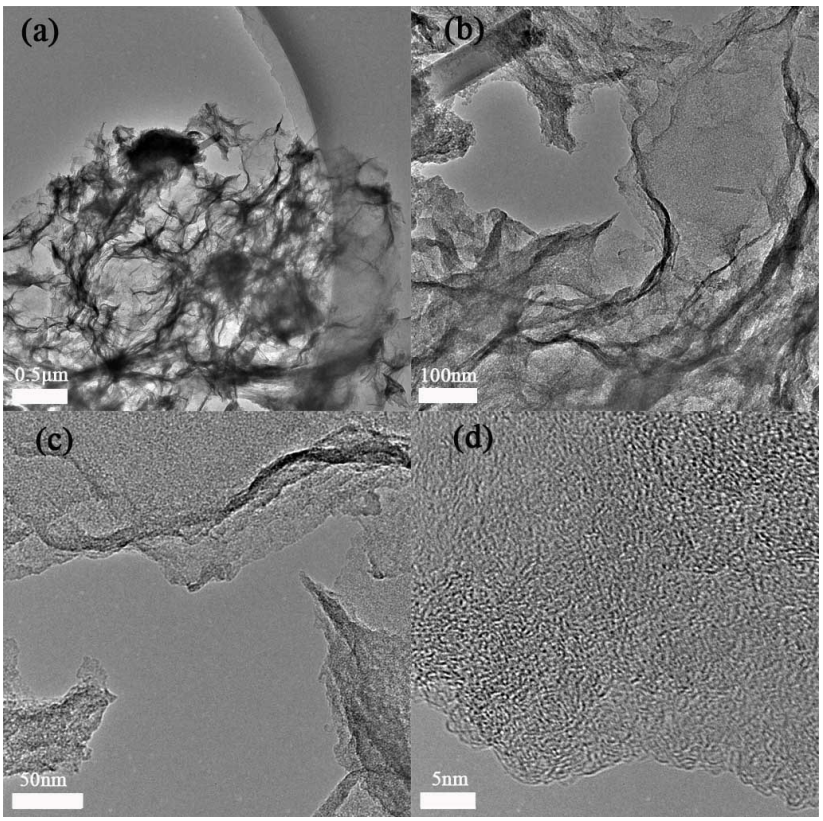

Fig. S2. TEM images of SNPC-700 with a scale bar of 0.5μm (a) , 100nm (b) ,50nm (c), 5nm(d).

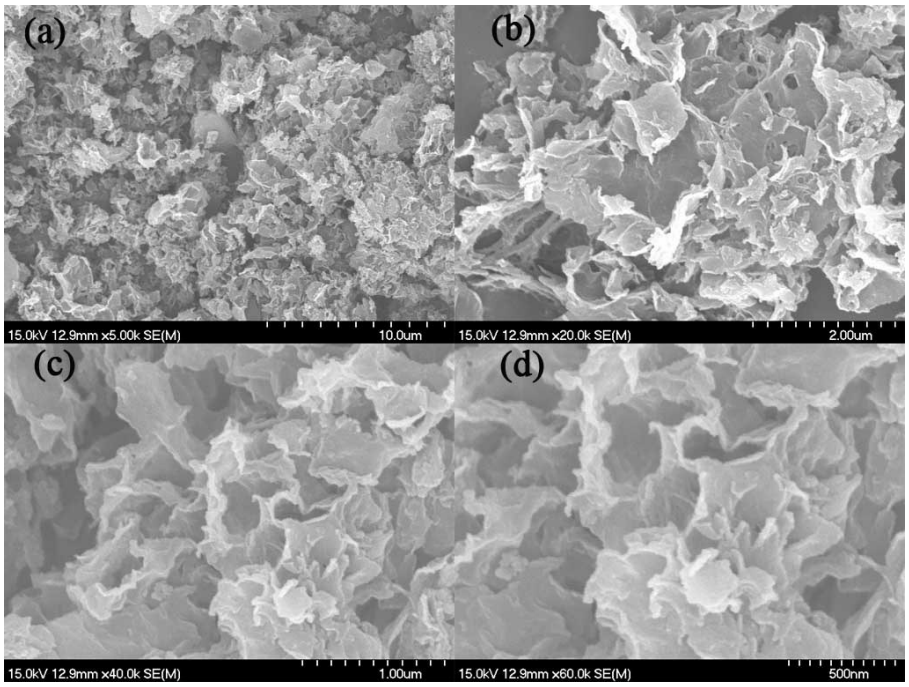

Fig. S3. SEM images of SNPC-700 with a scale bar of 10μm (a) , 2μm (b) ,1μm (c), 500nm(d).

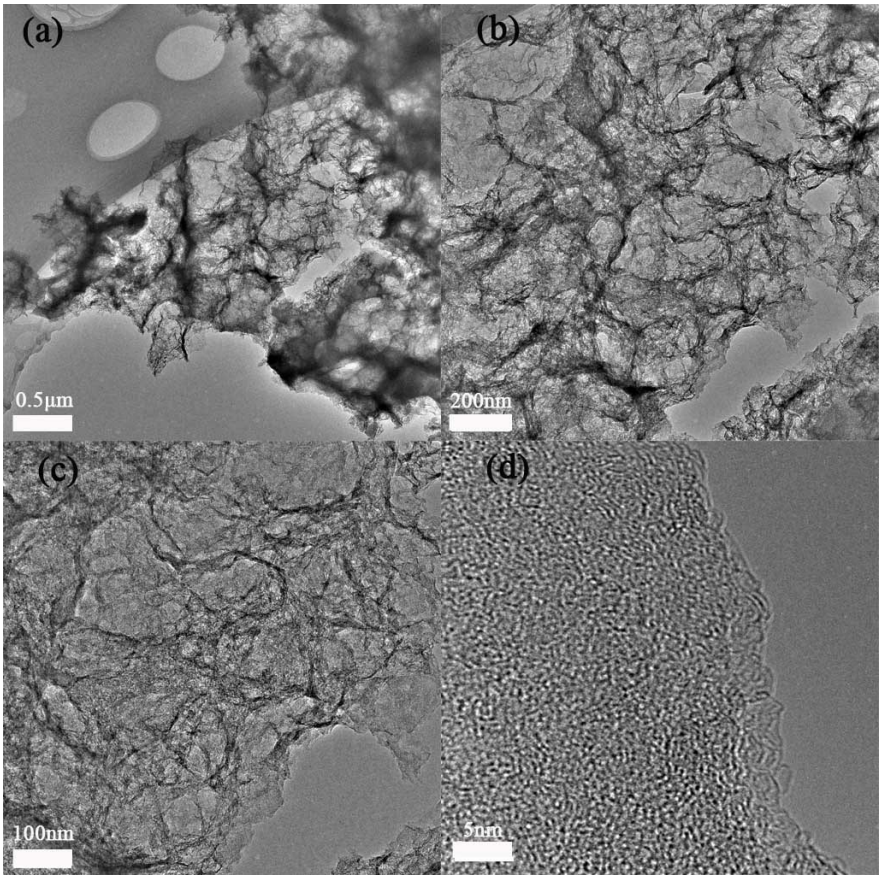

Fig. S4. TEM images of SNPC-600 with a scale bar of 0.5μm (a) , 200nm (b) ,100nm (c), 5nm(d).

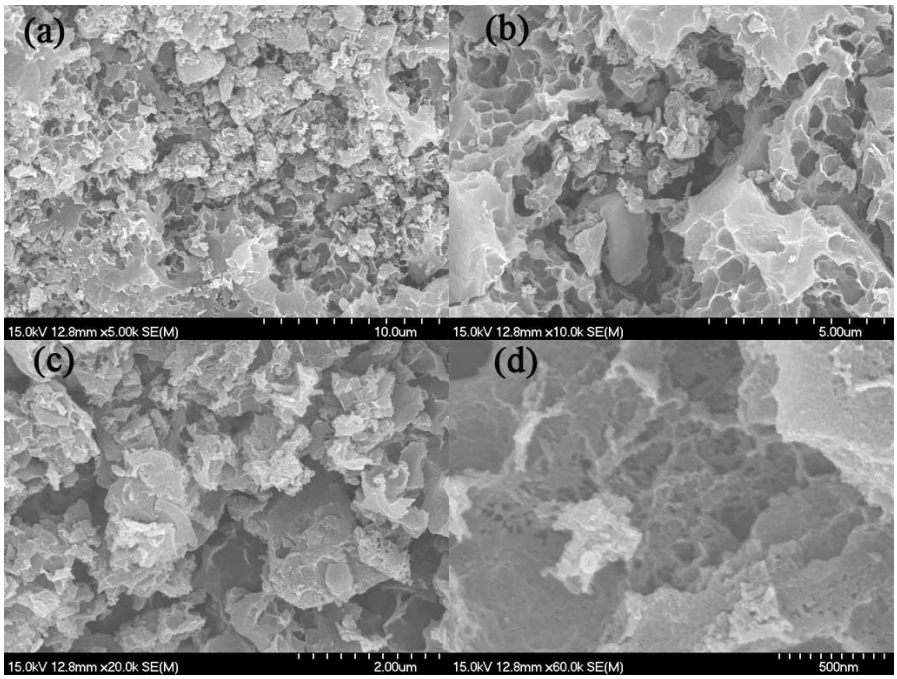

Fig. S5. SEM images of SNPC-600 with a scale bar of 10μm (a) , 5μm (b) ,2μm (c), 500nm(d).

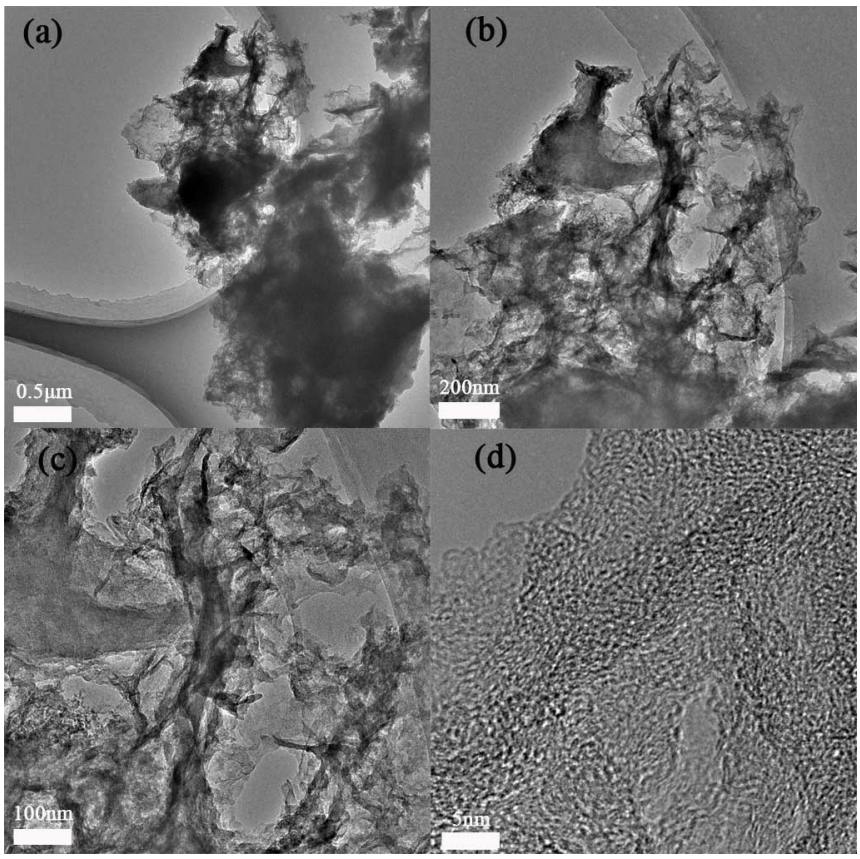

Fig. S6. (a-b) TEM images of SNPC-500 with a scale bar of 0.5μm (a) , 200nm (b) ,100nm (c), 5nm(d).

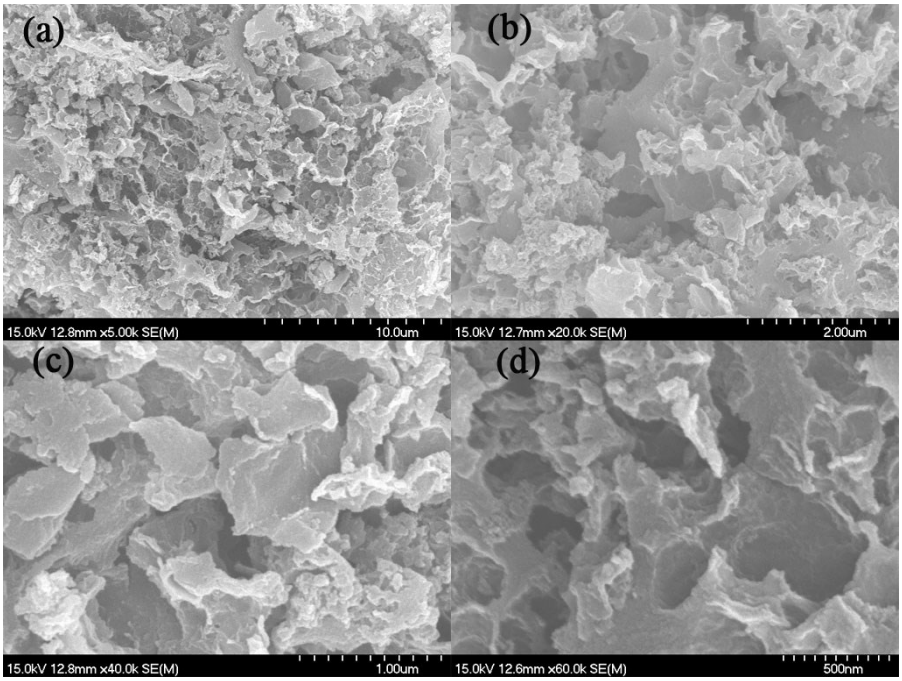

Fig. S7. SEM images of SNPC-500 with a scale bar of 10μm (a) , 2μm (b) ,1μm (c), 500nm(d).

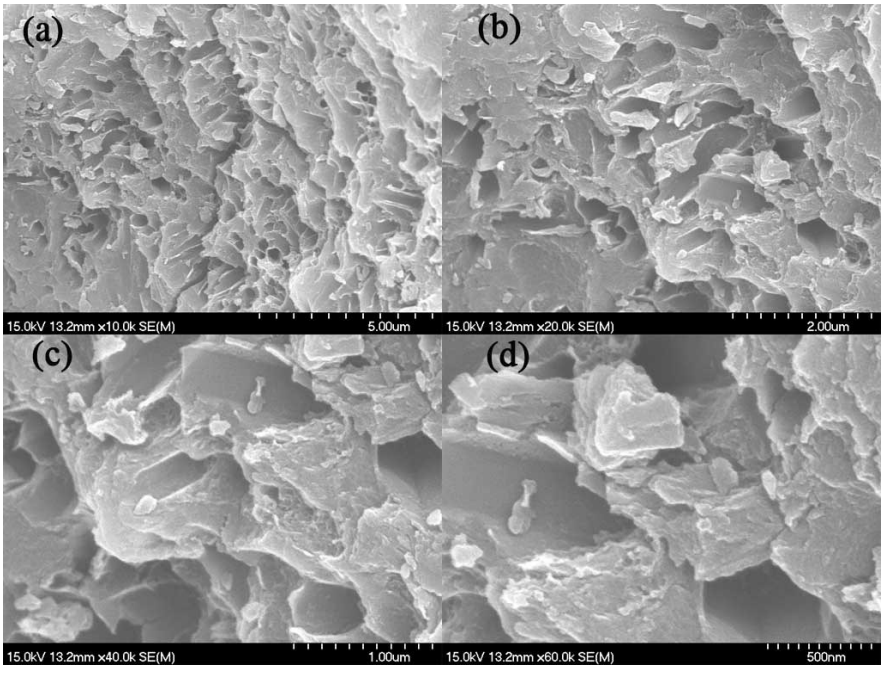

Fig. S8. SEM images of NPC-800 with a scale bar of 5μm (a) , 2μm (b) , 1μm (c), 500nm(d).

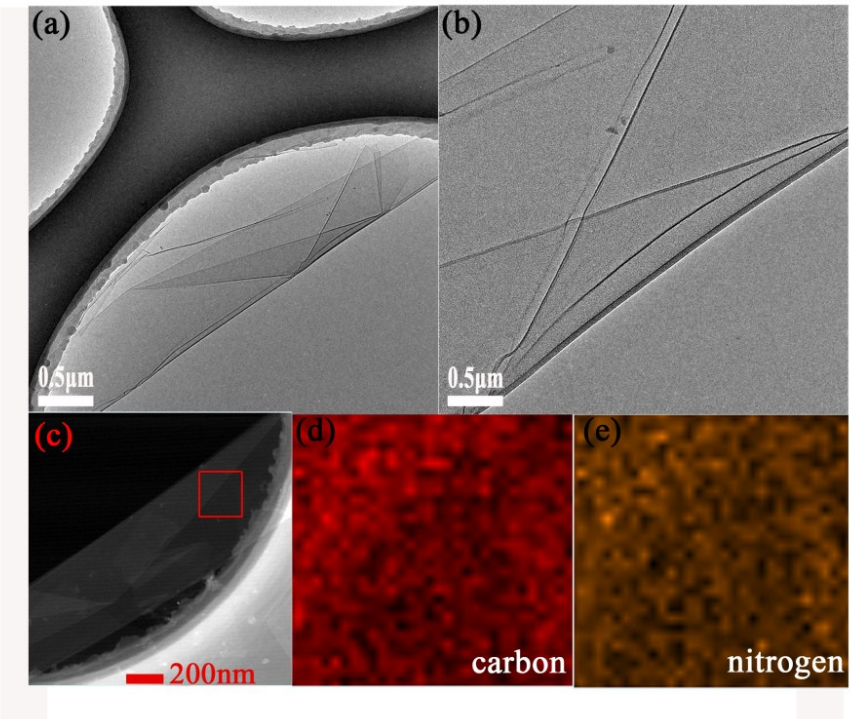

Fig. S9. (a-b) TEM images of NPC-800 with a scale bar of 0.5μm (c) TEM image of NPC-800. (d-e) EDX maps of NPC-800, C and N.

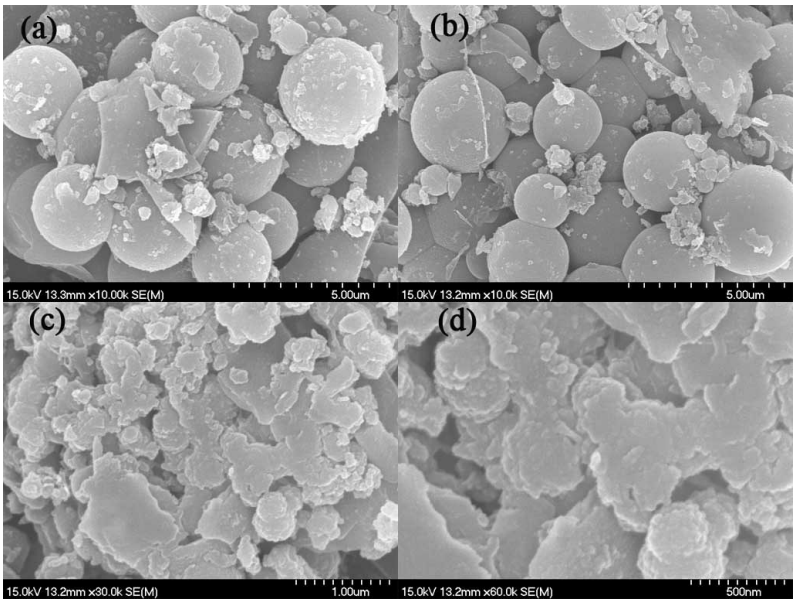

Fig. S10. SEM images of SPC-800 with a scale bar of 5μm (a-b) , 1μm (c), 500nm(d).

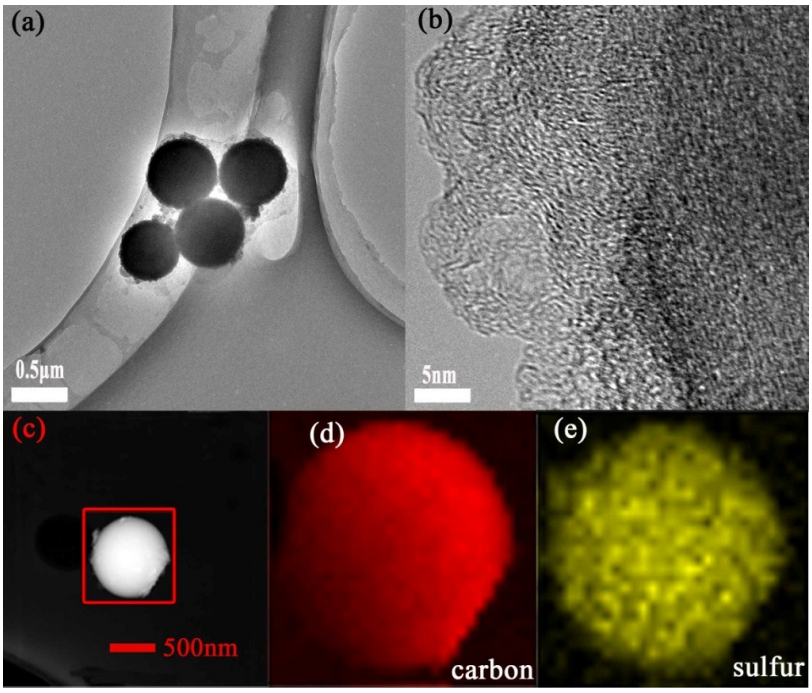

Fig. S11. (a-b) TEM images of NPC-800 with a scale bar of 0.5μm(a) , 5nm (b) , (c) TEM image of SPC-800. (d-e) EDX maps of SPC-800, C and S.

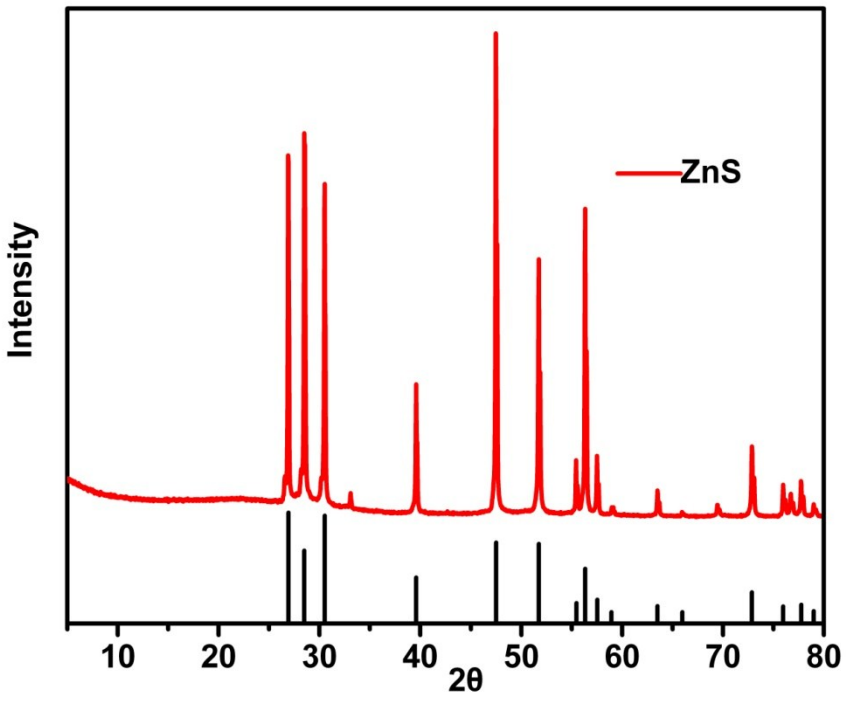

Fig.S12 XRD pattern of ZnS with PDF standard card (PDF NO.: 99-0109).

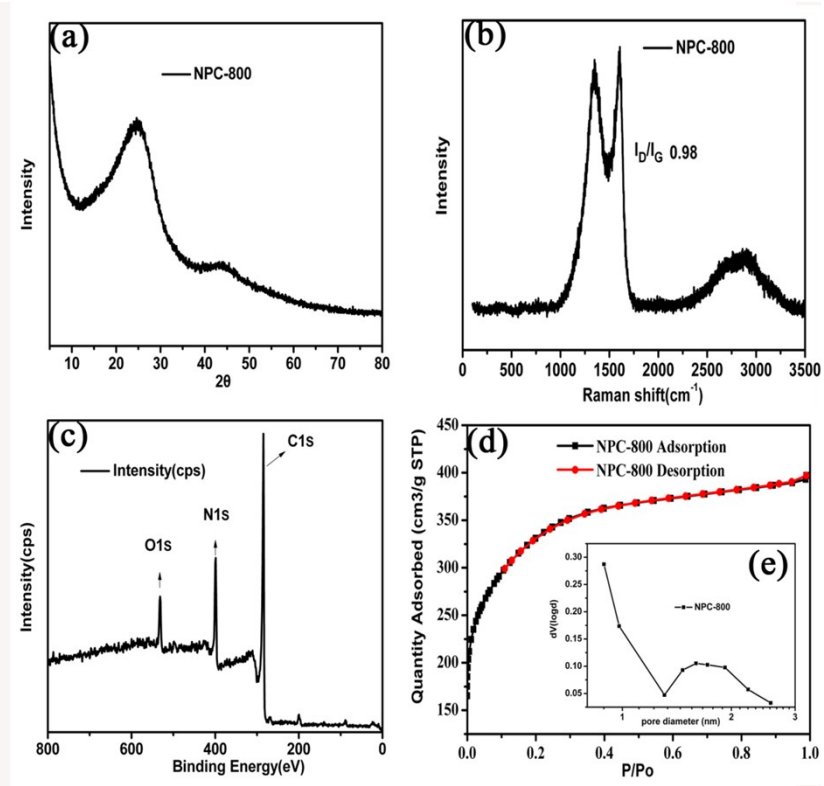

Fig. S13. (a) PXRD curves of the NPC-800. (b) Raman spectra of the NPC-800. (c) Survey XPS spectra of the NPC-800. (d) Nitrogen adsorption/desorption isotherms of NPC-800. (e) The pore size distribution of NPC-800.

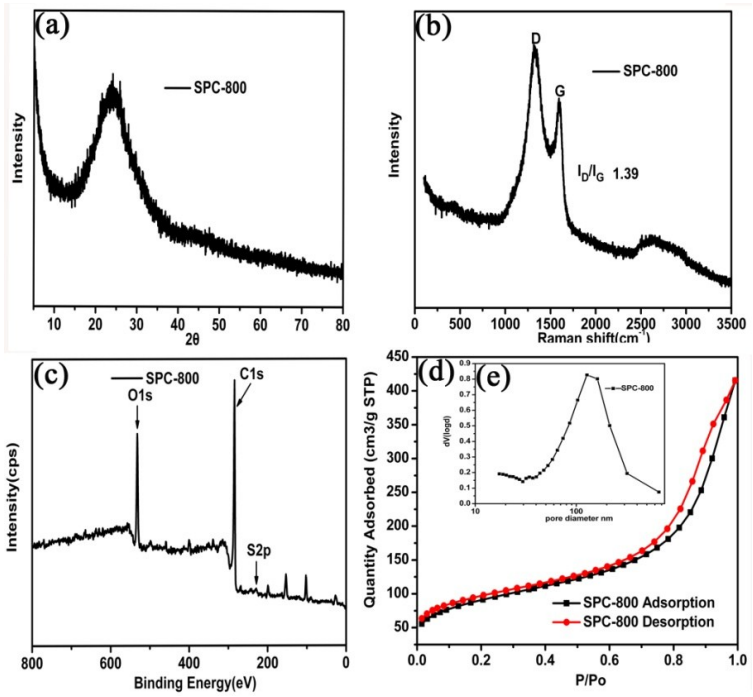

Fig. S14. (a) PXRD curves of the SPC-800. (b) Raman spectra of the SPC-800. (c) Survey XPS spectra of the SPC-800. (d) Nitrogen adsorption/desorption isotherms of SPC-800. (e) The pore size distribution of SPC-800.

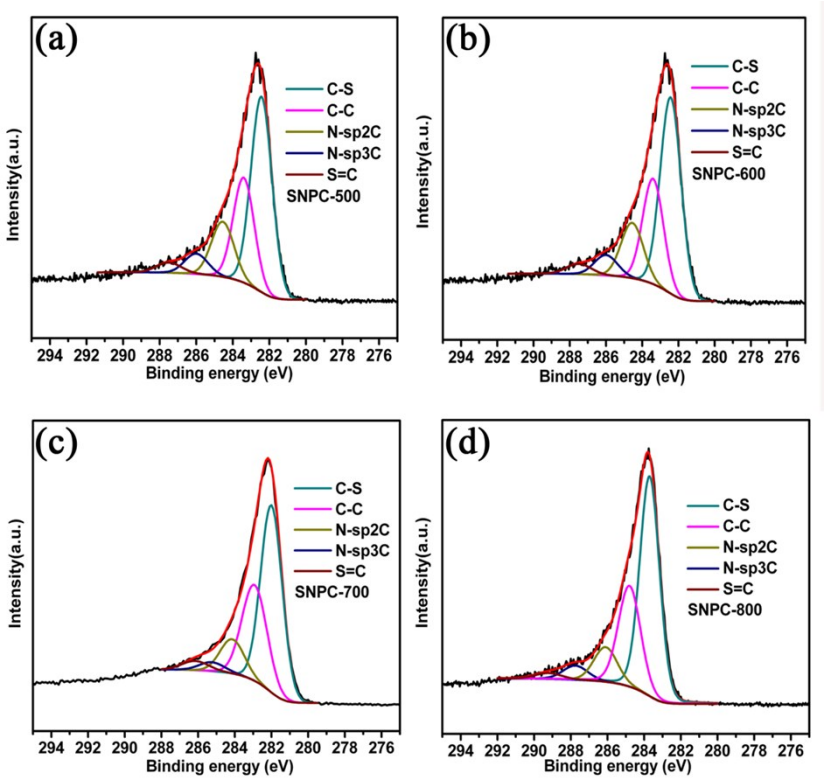

Fig. S15. (a) High resolution C1s XPS spectra of SNPC-500. (b) High resolution C1s XPS spectra of SNPC-600. (c) High resolution C1s XPS spectra of SNPC-700. (d) High resolution C1s XPS spectra of SNPC-800.

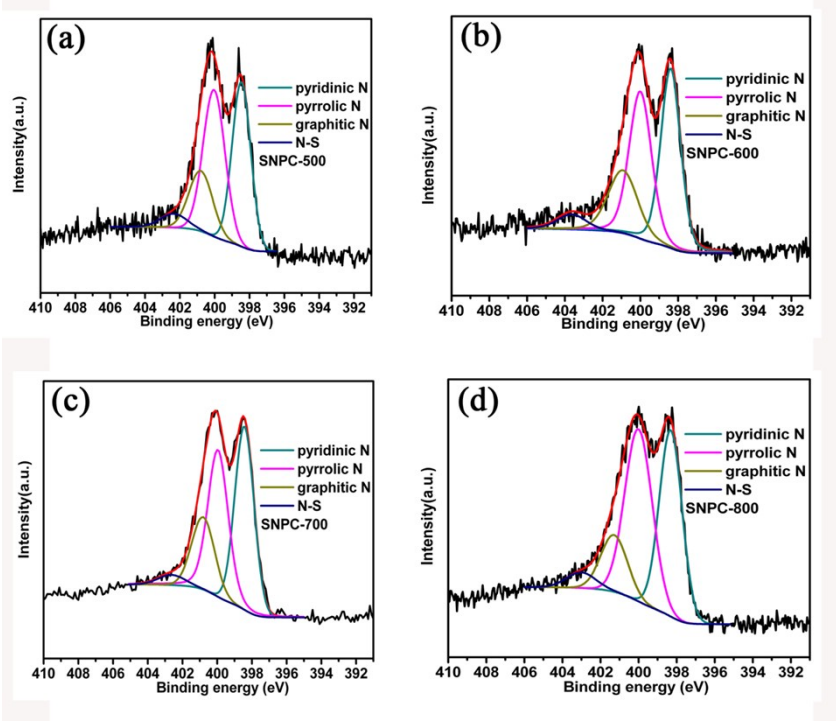

Fig. S16. (a) High resolution N1s XPS spectra of SNPC-500. (b) High resolution N1s XPS spectra of SNPC-600. (c) High resolution N1s XPS spectra of SNPC-700. (d) High resolution N1s XPS spectra of SNPC-800.

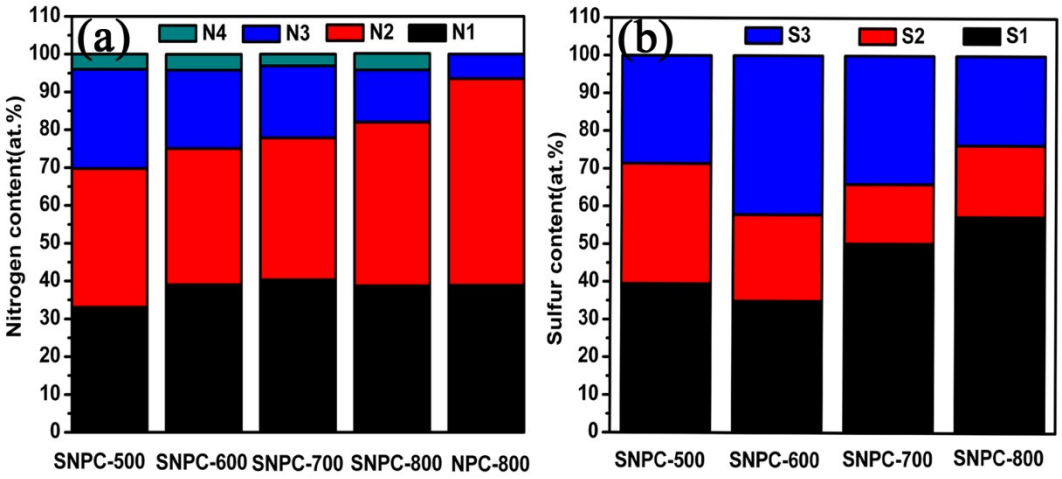

Fig. S17 (a) Atomic percentages of four nitrogen species for SNPC-500，SNPC-600 SNPC-700, SNPC-800 and NPC-800 derived from XPS analysis. (b) Atomic percentages of three sulfur species for SNPC-500，SNPC-600 SNPC-700, and SNPC-800 derived from XPS analysis.

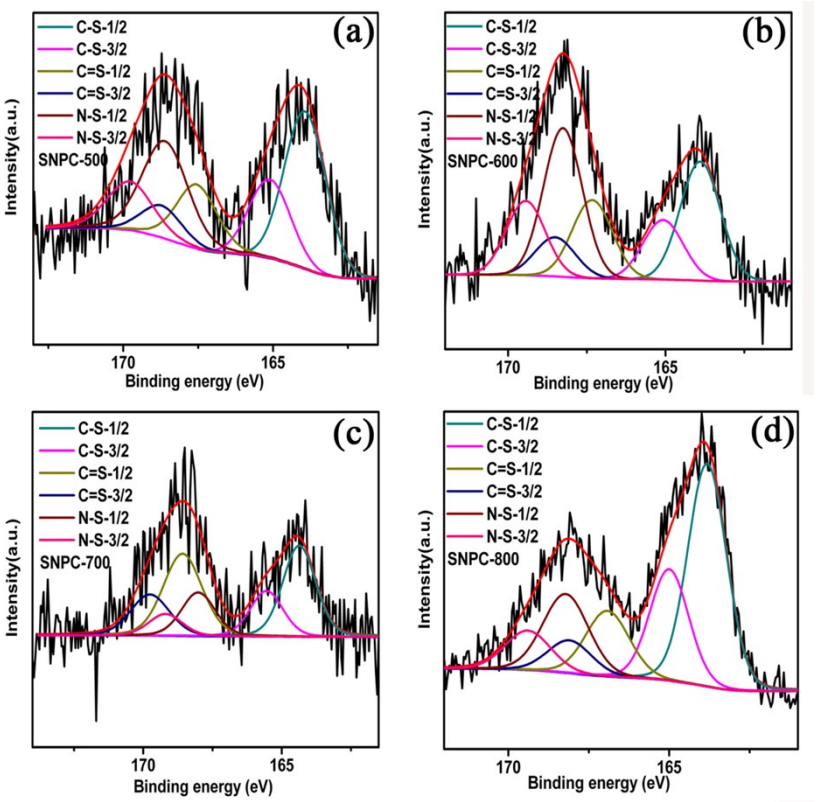

Fig. S18. (a) High resolution S2p XPS spectra of SNPC-500. (b) High resolution S2p XPS spectra of SNPC-600. (c) High resolution S2p XPS spectra of SNPC-700. (d) High resolution S2p XPS spectra of SNPC-800.

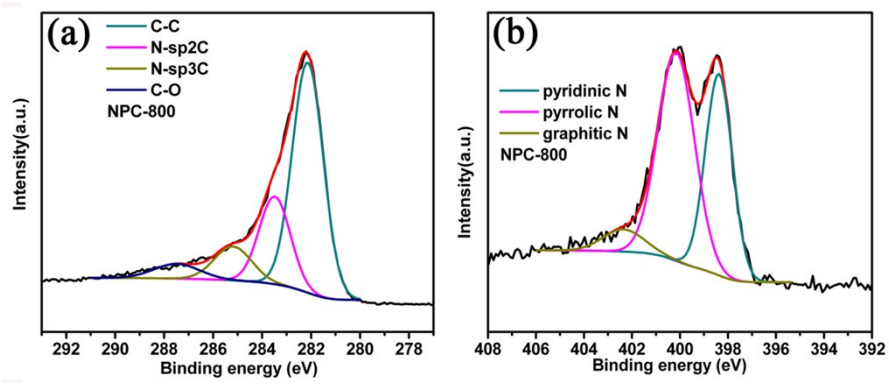

Fig. S19 (a) High resolution C1s XPS spectra of NPC-800. (b) High resolution N1s XPS spectra of NPC-800.

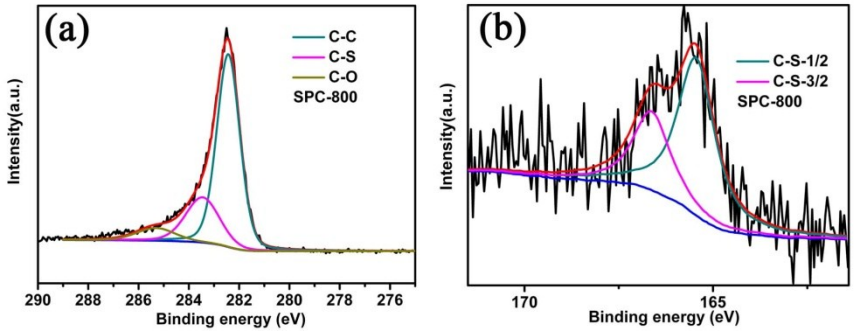

Fig. S20 (a) High resolution C1s XPS spectra of SPC-800. (b) High resolution S2p XPS spectra of SPC-800.

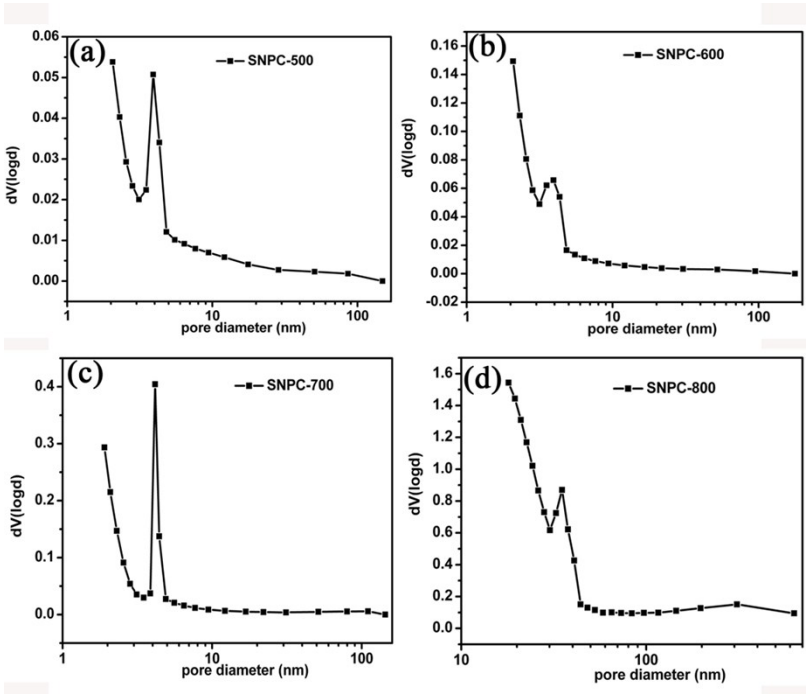

Fig. S21 the pore size distribution of SNPC-500(a)，SNPC-600(b)，SNPC-700(c) and SNPC-800(d), respectively.

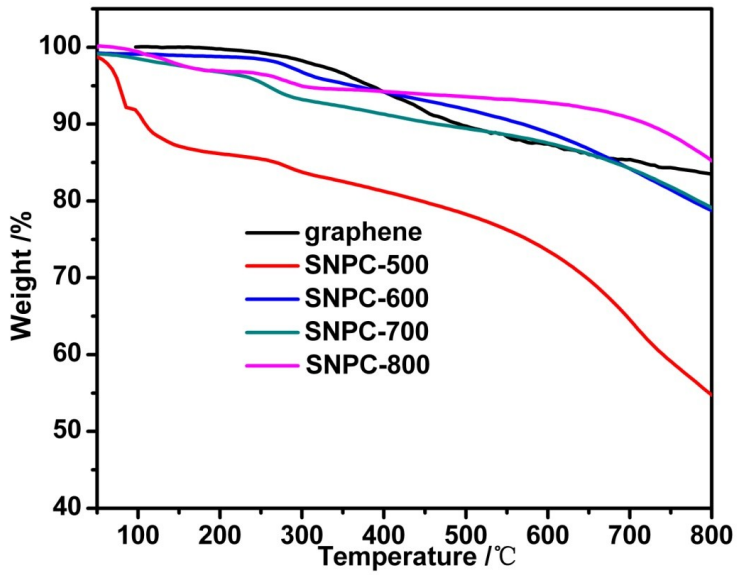

Fig. S22. TG curves of SNPC-500, SNPC-600, SNPC-700,and SNPC-800.

Table S1 result of EA and XPS for NPC-800, SPC-800, SNPC-500, SNPC-600, SNPC-700 and SNPC-800

	Elemental analysis(wt%)				XPS(mas%)		
	N	C	S	H	C	N	S
SNPC-500	16.93	47.84	0.79	2.48	73.65	25.16	1.18
SNPC-600	20.05	51.17	1.75	3.39	72.71	25.45	1.84
SNPC-700	21.06	52.59	2.36	3.03	76.68	19.43	1.13
SNPC-800	14.82	60.30	3.86	2.36	85.24	12.36	2.40
NPC-800	13.62	43.87	0.00	3.95	66.50	24.42	0.00
SPC-800	0.00	54.64	2.93	3.82	78.44	0.00	1.45

2. ORR measure results.

In the rotating-disk electrode (RDE) tests, the linear sweep voltammograms (LSVs) were measured in O_2 saturated 0.1 M KOH solution and the potential was varied from 0.1 to -0.8V(vs. Ag/AgCl/V) with a scan rate of 10 mV s^{-1} at various rotating speeds from 400 to 2025 rpm.

To further study the ORR performance, the number of electron (n) was conducted according to Koutecky-Levich (K-L) equation:

$$j^{-1} = j_L^{-1} + j_k^{-1} = (B\omega 1/2)^{-1} + j_k^{-1} \quad (1)$$

$$B = 0.62\, n\, F\, C_0\, (D_0)^{2/3} \nu^{-1/6} \quad (2)$$

$$J_k^{-1} = J^{-1} - (0.62nF\, C_0\, (D_0^{2/3} \nu^{-1/6} \omega^{1/2})^{-1} \quad (3)$$

Where j is the measured current density, J_k and j_L are the kinetic and diffusion-limiting current density, respectively. B is Levich slope which is given by (2). n is the number of electrons transferred for ORR. ω is the rotation rate ($\omega = 2\pi N$, N is the linear rotation speed), F is the Faraday constant (F = 96485 C mol^{-1}), ν is the kinetic viscosity, and C_0 is the concentration of O_2 ($1.2*10^{-3}$ mol L^{-1}), and C_0 is the diffusion coefficient of O_2 in 0.1 M KOH ($1.9*10^{-5}$ cm s^{-1}). According to Equations (1) and (2), the number of electrons transferred (n) can be calculated to be 4.1 , 4.2, 2.2 and 2.3 for SNPC-800，Pt/C (20 % loading) , NPC-800 and SPC-800 , respectively , which indicates that the SNPC-800 and Pt/C lead to a four-electron-transfer reaction to reduce directly oxygen into OH^-，however，NPC-800 and SPC-800 lead to a two-electron-

transfer reaction to reduce directly oxygen into O_2^{2-}.

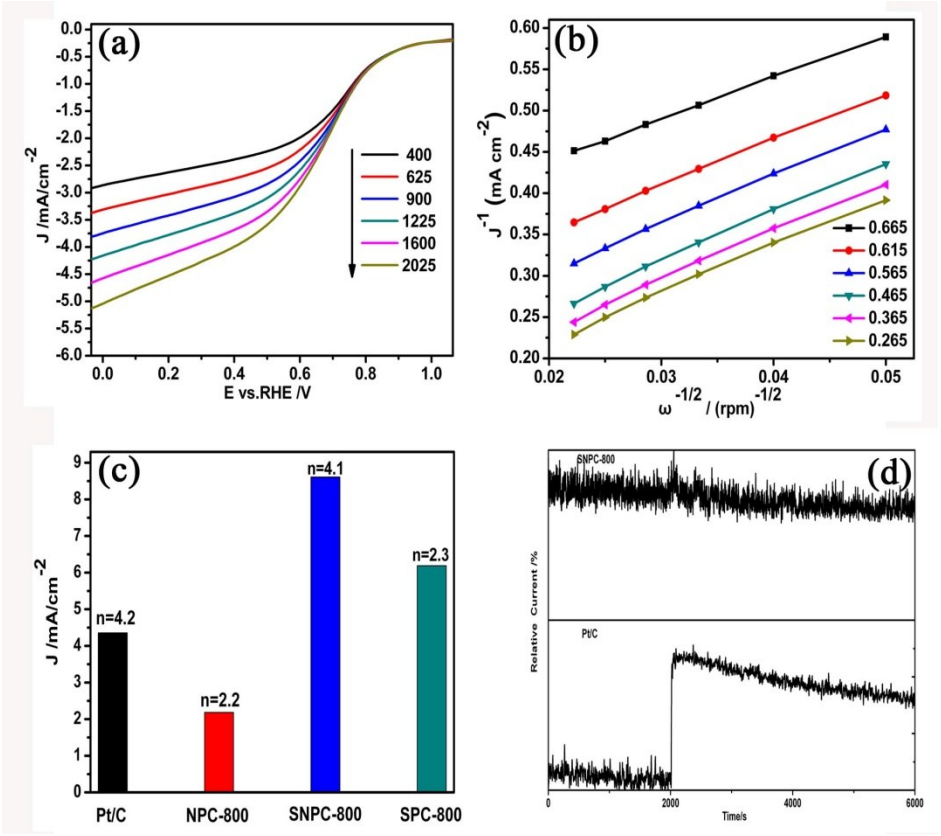

Fig. S23. (a) SNPC-800 on RDE at different rotating rates (400 to 2,025 rpm) in O_2 saturated 0.1 M KOH. (b) Koutecky-Levich plots of SNPC-800 . (c) Electrochemical activity given as the kinetic-limiting current density (J_k) at -0.6 V (vs.Ag/AgCl/V) for the SNPC-800, NPC-800 ,SPC-800 supported on GC electrode in comparison with that of commercial Pt/C (20 % loading) catalyst. (d) methanol crossover evaluation from the i−t chronoamperometric response in aqueous solution of KOH.

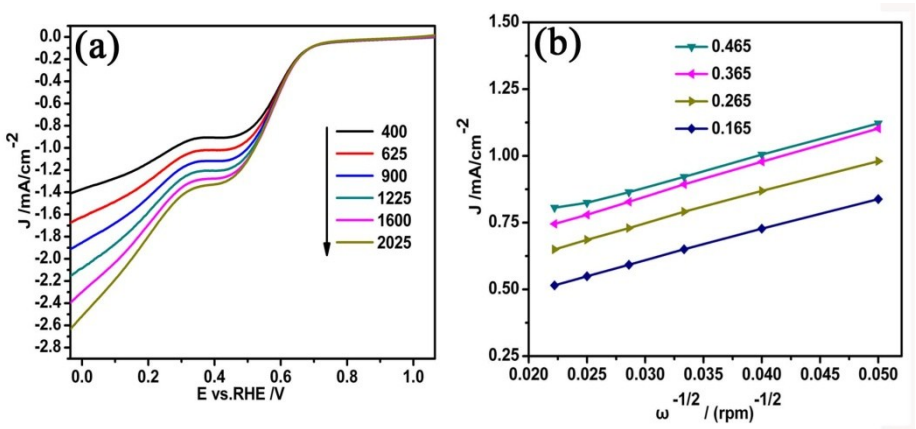

Fig. S24. (a) NPC-800 on RDE at different rotating rates (400 to 2,025 rpm) in O_2-saturated 0.1 M KOH. (b) Koutecky-Levich plots of NPC-800 .

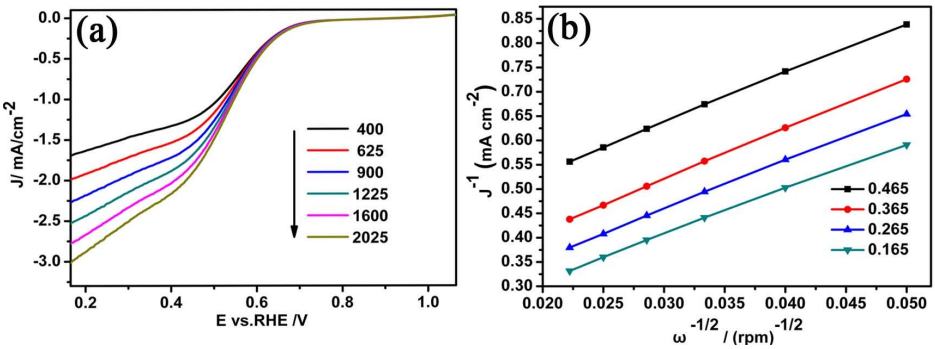

Fig. S25. (a) SPC-800 on RDE at different rotating rates (400 to 2,025 rpm) in O_2-saturated 0.1 M KOH. (b) Koutecky-Levich plots of SPC-800 .

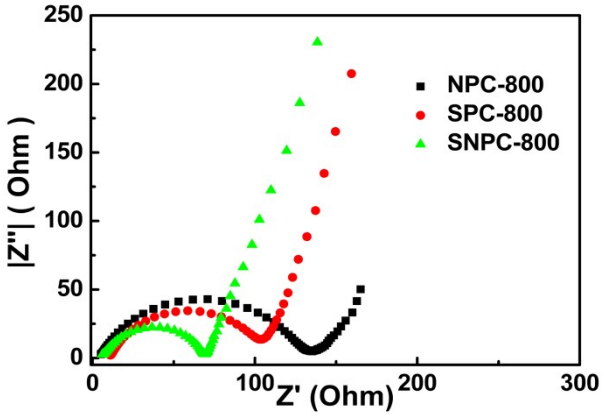

Fig. S26 impedance spectra of SNPC-800, SPC-800 and NPC-800.

3. Li-ion battery property of SNPC-800，NPC-800 and SPC-800.

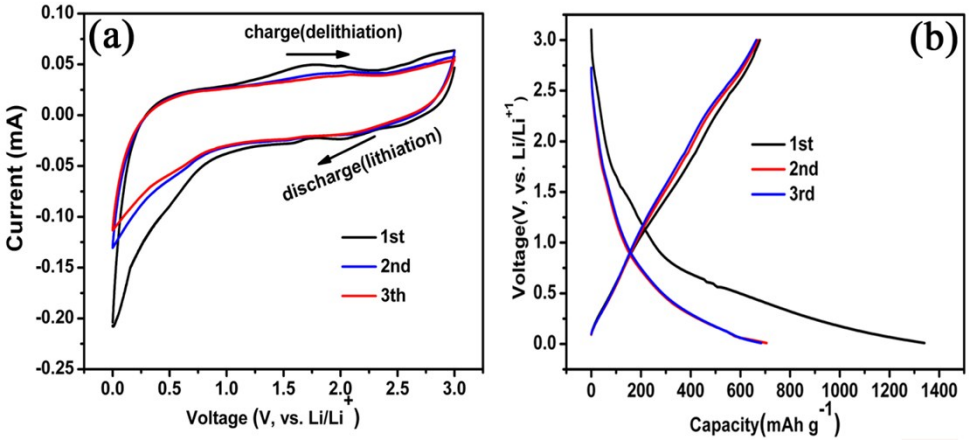

Fig. S27. Electrochemical properties of the as-prepared samples. (a) CV curves of sample SNPC-800 scanned between 0.0 and 3.0 V at a rate of 0.1 mVs^{-1}. (b) charge/discharge profiles of sample SNPC-800 at different cycles with a current densities of 100 mA g^{-1}.

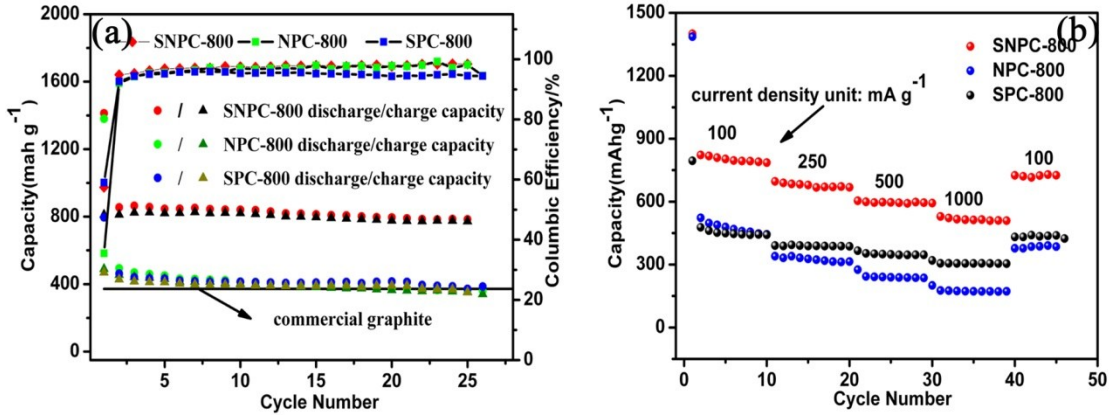

Fig. S28. LIB properties of the as-prepared samples. (a) Cycling performance and Coulombic efficiency of samples SNPC-800 , SPC-800 and NPC-800 at a 100 mA g^{-1} current density. (b) Rate performance of samples SNPC-800, SPC-800 and NPC-800 (without Super P).

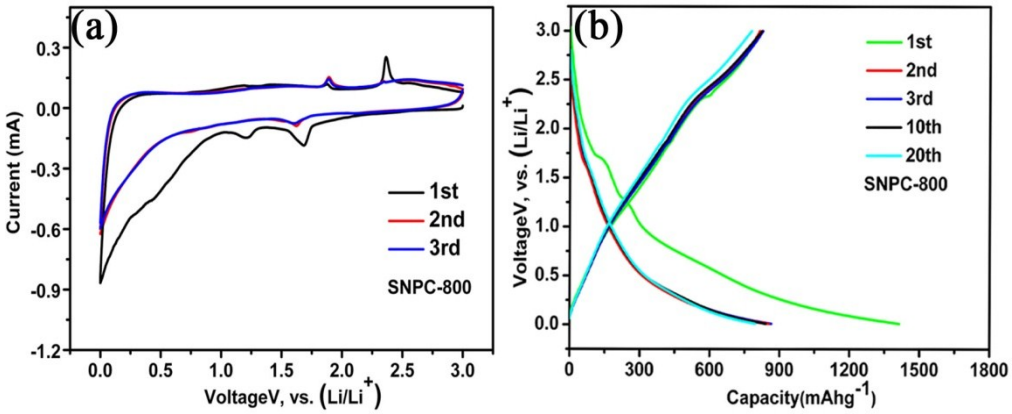

Fig. S29 . Electrochemical properties of the as-prepared samples. (a) CV curves of sample SNPC-800 scanned between 0.0 and 3.0 V at a rate of 0.1 mVs^{-1}. (b) charge/discharge profiles of sample SNPC-800 at different cycles with a current densities of 100 mA g^{-1} (without Super P) .

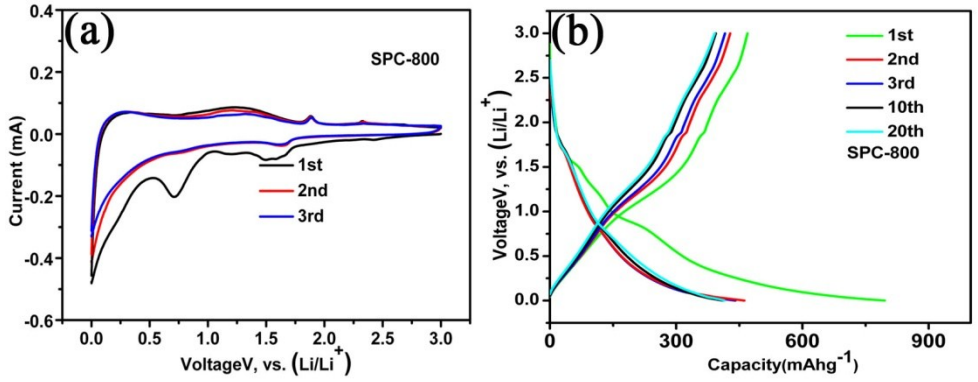

Fig. S30 . Electrochemical properties of the as-prepared samples. (a) CV curves of sample SPC-800 scanned between 0.0 and 3.0 V at a rate of 0.1 mVs^{-1}. (b) charge/discharge profiles of sample SPC-800 at different cycles with a current densities of 100 mA g-1 (without Super P) .

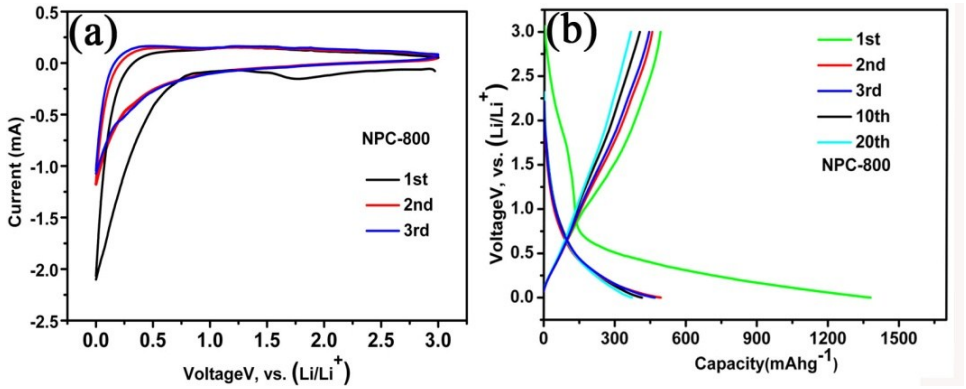

Fig. S31. Electrochemical properties of the as-prepared samples. (a) CV curves of sample NPC-800 scanned between 0.0 and 3.0 V at a rate of 0.1 mVs^{-1}. (b) charge/discharge profiles of sample NPC-800 at different cycles with a current densities of 100 mA g-1 (without Super P) .

4. DFT calculation results for ORR catalytic mechanism

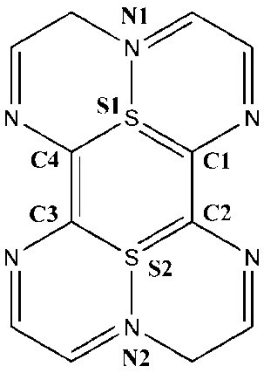

Scheme 1 the sketch of fragment of SNPC structure

Table S2 bader charge of SNPG, O-SNPG,HO-SNPG and HOO-SNPG

	C1	C2	C3	C4	N1	N2	S1	S2	O
SNPG	0.35	0.32	0.27	0.37	−1.08	−1.15	0.26	0.26	–
O-SNPG	0.57	0.49	0.59	0.58	−1.07	−1.11	−0.91	−0.53	0.60
HO-SNPG	0.27	0.71	0.25	0.23	−1.15	−1.16	0.18	0.28	-1.10
HOO-SNPG	0.30	0.67	0.29	0.33	−1.10	−1.16	0.24	0.30	-0.51

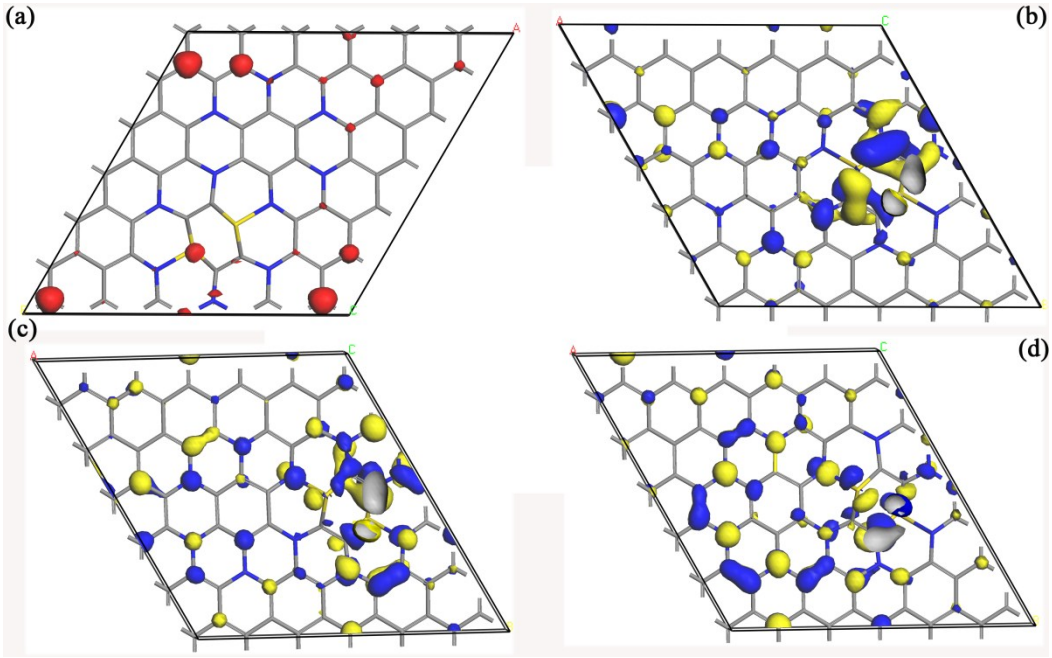

Fig. S32 (a)spin density diagram of SNPC (red); (b) HOMO, (c) LUMO and (d) HOMO-1 of SNPC.

Figure.S33 the product in the salt of $NiCl_2$ (left) and $CoCl_2$ (right)